



Nanoparticles With Affinity for α -Synuclein Sequester α -Synuclein to Form Toxic Aggregates in Neurons With Endolysosomal Impairment

Peizhou Jiang^{1*}, Ming Gan², Shu-Hui Yen¹ and Dennis W. Dickson^{1*}

¹ Department of Neuroscience, Mayo Clinic, Jacksonville, FL, United States, ² Department of Laboratory Medicine and Pathology, Mayo Clinic, Jacksonville, FL, United States

OPEN ACCESS

Edited by:

Neha Gogia,
Yale University, United States

Reviewed by:

Maria Xilouri,
Biomedical Research Foundation
of the Academy of Athens (BRFAA),
Greece

Francesca Longhena,
University of Brescia, Italy

*Correspondence:

Peizhou Jiang
Jiang.peizhou@mayo.edu
Dennis W. Dickson
dickson.dennis@mayo.edu

Specialty section:

This article was submitted to
Brain Disease Mechanisms,
a section of the journal
Frontiers in Molecular Neuroscience

Received: 09 July 2021

Accepted: 21 September 2021

Published: 20 October 2021

Citation:

Jiang P, Gan M, Yen S-H and
Dickson DW (2021) Nanoparticles
With Affinity for α -Synuclein
Sequester α -Synuclein to Form Toxic
Aggregates in Neurons With
Endolysosomal Impairment.
Front. Mol. Neurosci. 14:738535.
doi: 10.3389/fnmol.2021.738535

Parkinson's disease (PD) is one of the most common neurodegenerative diseases. It is characterized pathologically by the aggregation of α -synuclein (α S) in the form of Lewy bodies and Lewy neurites. A major challenge in PD therapy is poor efficiency of drug delivery to the brain due to the blood–brain barrier (BBB). For this reason, nanomaterials, with significant advantages in drug delivery, have gained attention. On the other hand, recent studies have shown that nanoparticles can promote α S aggregation in salt solution. Therefore, we tested if nanoparticles could have the same effect in cell models. We found that nanoparticle can induce cells to form α S inclusions as shown in immunocytochemistry, and detergent-resistant α S aggregates as shown in biochemical analysis; and nanoparticles of smaller size can induce more α S inclusions. Moreover, the induction of α S inclusions is in part dependent on endolysosomal impairment and the affinity of α S to nanoparticles. More importantly, we found that the abnormally high level of endogenous lysosomotropic biomolecules (e.g., sphingosine), due to impairing the integrity of endolysosomes could be a determinant factor for the susceptibility of cells to nanoparticle-induced α S aggregation; and deletion of GBA1 gene to increase the level of intracellular sphingosine can render cultured cells more susceptible to the formation of α S inclusions in response to nanoparticle treatment. Ultrastructural examination of nanoparticle-treated cells revealed that the induced inclusions contained α S-immunopositive membranous structures, which were also observed in inclusions seeded by α S fibrils. These results suggest caution in the use of nanoparticles in PD therapy. Moreover, this study further supports the role of endolysosomal impairment in PD pathogenesis and suggests a possible mechanism underlying the formation of membrane-associated α S pathology.

Keywords: α -synuclein, aggregation, endolysosomal impairment, Parkinson's disease, GBA

INTRODUCTION

Parkinson's disease (PD) is the second most common age-related neurodegenerative disease worldwide (Mhyre et al., 2012). Pathologically, PD is characterized by the loss of dopaminergic neurons in the substantia nigra and by intraneuronal α -synuclein (α S) aggregates in the form of Lewy bodies and Lewy neurites (Mhyre et al., 2012). Although the restoration of dopaminergic neurotransmission and alleviation of burden of α S have been considered as two key strategies for

PD therapy (Meissner et al., 2011; Mhyre et al., 2012), there is still no cure for this disease. This is in part due to the presence of the blood–brain barrier (BBB), which reduces the efficiency of drug delivery to the brain. It may also be due to a decreased biological activity of the drug resulting from enzymatic degradation or other factors encountered by the drug during its delivery (Gavhane and Yadav, 2012; Hersh et al., 2016; Raza et al., 2019). In this regard, nanoparticles, due to their unique properties in size and biodegradability (Mahapatro and Singh, 2011; Shang et al., 2014; Hoshyar et al., 2016), as well as their BBB permeability and drug loading capacity (Shen et al., 2017; Teleanu et al., 2018), have attracted attention as a drug-delivery approach in PD (Leyva-Gomez et al., 2015; Lafuente et al., 2019).

On the other hand, some nanoparticles that have been suggested for drug delivery (Murthy, 2007) have been shown to induce fibrillization of aggregation-prone proteins (Linse et al., 2007; D’Onofrio et al., 2020). For example, recombinant soluble α S in salt solution has been induced to form aggregates upon the addition of nanoparticles (Alvarez et al., 2013; Mohammadi and Nikkhah, 2017; Tahaei Gilan et al., 2019). Some of those aggregates were cytotoxic to cultured neuronal cells (Tahaei Gilan et al., 2019). Since endocytosis is a major pathway in nano-based drug delivery to cells (Behzadi et al., 2017), we were interested in determining if nanoparticles can directly interact with cytoplasmic α S in neuron cells, and if this interaction can induce α S to form neurotoxic aggregates. Our results not only pointed out a potential risk of nanoparticles in PD treatment but also revealed a possible mechanism underlying the formation of membrane-associated α S pathology in PD.

MATERIALS AND METHODS

Cell Culture and Maintenance

Cell cultures in this study included transfectants derived from human H4 neuroglioma: “H4/V1S:SV2,” “H4/CBD-V1S:SV2-CBD,” “H4/V1S:SV2/LAMP1-eCFP/mCherry-galactin-3,” and a transfectant from BE(2)-M17 neuroblastoma cells—“3D5.” The purpose of using each cell line was described in the section of Results. All cell lines were maintained in OPTI-MEM (Invitrogen) medium containing 10% fetal bovine serum (Invitrogen) at 37°C with 5% CO₂ and 100% humidity. For live cell imaging with confocal microscopy, cells were cultured in Nunc® Lab-Tek® II chambered coverglass (Sigma-Aldrich). For the differentiation of human dopaminergic cell line BE(2)-M17-derived cells, the medium was replaced with Neurobasal medium (Invitrogen), 2% B-27 supplement (Invitrogen), 2 mM L-glutamine (Sigma-Aldrich), and 10 μ M retinoic acid (Sigma-Aldrich).

Lentiviral Plasmids and Virus Preparation

Lentiviral plasmids carrying LAMP1-eCFP and mCherry-galactin-3 were described previously (Jiang et al., 2017). The lentiviral vector for CRISPR-Cas9 knockout of GBA1 was designed by VectorBuilder Inc. (**Supplementary Figure 2**). The sequences of two single guide RNAs (sgRNAs) were “AGACCAATGGAGCGGTGAAT” and “TGTGGTGAGTACT

GTTGGCG,” respectively. The protocols used for the preparation of lentivirus carrying genes of interest were the same as described previously (Jiang et al., 2013).

Nanoparticle Preparation

Commercially available nanoparticles were Gold (Nanocs), TiO₂ (US Research Nanomaterials), ZnO (Inframat), Fe₃O₄ (US Research Nanomaterials), and SiO₂ (US Research Nanomaterials). The Alexa Fluor™ 647-labeled SiO₂ nanoparticles were customized product (30 nm) from Nanocs. The chitin nanoparticles were customized (80 nm) from Nanoshel. To prepare fresh concentrated nanoparticle solutions, the original powder was weighed and added into 1 \times PBS, then sonicated for 5 min at maximal power (Sonicator 3000, Misonix). The concentrated nanoparticle solution was further diluted into culture media to make final nanoparticle-supplemented media, which were sonicated for at least 1 min before cell treatment.

Nanoparticle Treatment and Quantification of Induced α S Inclusions in Cells

Cells were plated on coverglass with 8-well culture chamber at the same density overnight, then treated with different nanoparticles. The next day, the cells were exposed to 1 mM lysosomotropic detergent [L-leucyl-L-leucine methyl ester (LLME)] (Cayman Chemical) for 1–2 h to induce endolysosomal rupture. In parallel, sibling cultures without nanoparticles or LLME treatment were set as two different negative controls. After fixation with 4% paraformaldehyde (PFA), cells with and without α S inclusions were evaluated and photographed under a confocal microscope (Zeiss LSM 510, Carl Zeiss MicroImaging). For measuring the ratio of cells bearing α S inclusions, five fields (upper right, upper left, center, lower right, and lower left) with at least 90 cells were selected from each group for cell count.

Separation of Detergent-Soluble and Insoluble Fractions

Neuroblastoma BE(2)-M17D-derived cell model—3D5 (Ko et al., 2008) were differentiated and induced to express human wild-type α S, then exposed to media supplemented with and without SiO₂ nanoparticles for 1 day, followed by the induction of endolysosomal membrane rupture for 1–2 h. Cells were then harvested for protein extraction by extraction buffer [1% Triton X-100 (Tx) and 1% (v/v) protease inhibitor cocktail (Sigma) in 1 \times PBS] to obtain Tx-soluble and Tx-insoluble fractions following a previous protocol (Bae et al., 2015). The same amount of proteins from different groups was mixed with loading buffer and then resolved by sodium dodecyl-sulfate polyacrylamide gel electrophoresis (SDS-PAGE) followed by the Western blotting.

Assay Comparing α S Binding Affinity for Different Nanoparticles

The method for detecting the binding affinity of nanoparticles to α S was similar to that reported in a previous study (Hata et al., 2014) with minor modifications. Freshly prepared recombinant α S solution was mixed with different nanoparticles to get a final

concentration of 0.5 $\mu\text{g}/\mu\text{l}$ for αS and 200 $\mu\text{g}/\text{ml}$ for both SiO_2 and chitin, respectively. A tube of αS solution with the same concentration of αS but without mixing with any nanoparticle was included as a control (Con). All samples were incubated at 37°C for 1 h with constant rotating. The αS protein bound to nanoparticles was isolated by centrifugation at $30,000 \times g$ for 20 min at 4°C. The top layer of supernatant was removed to a new tube for measuring the concentration remained in solutions. The pellets containing a mixture of nanoparticles and particle-bound αS were washed with 1 ml PBS and centrifuged again for three times to remove residual unbound αS protein, then mixed with 10% SDS buffer, followed by the addition of an equal amount of Laemmli sample buffer (Bio-Rad Laboratories) and boiled for 5 min at 95°C. The boiled samples were centrifuged, and the supernatants were used for SDS-PAGE. The gels were subjected to silver staining to show the bound αS in each group. A tube containing αS solution was saved before mixing with nanoparticles and used as a negative control.

Sphingosine Measurement in Cell Cultures

Pellets of cultured cells (comparable cell number per group) were resuspended in $1 \times \text{PBS}$ and then lysed by ultrasonication four times, followed by centrifugation at $1,500 \times g$ for 10 min at 4°C. Supernatants collected from cultured cells were used for measuring the concentration of sphingosine according to the manufacturer's instructions (Sphingosine ELISA Kit Lifespan Biosciences). Briefly, samples were added to a plate, followed by the addition of detection reagent A and 1 h of incubation at 37°C. After incubation, the reagents in the plate were removed and the plate was washed completely with buffer and then loaded with detection reagent B for 45 min of incubation at 37°C. At the end of incubation, sample wells were emptied and washed again, then loaded with TMB substrate for 10–20 min of incubation at 37°C, followed by the addition of stop solution and the measurement of optical density by a microplate reader (SpectraMax Paradigm, Molecular Devices).

Immunocytochemistry

Cells were rinsed with $1 \times \text{PBS}$, fixed in 4% PFA, and permeabilized with 0.1 M Tris-buffered saline (TBS; pH 7.6) containing 0.5% Triton X-100 for 5 min, then blocked with 3% goat serum in TBS, incubated with the primary antibody in TBS containing 1% goat serum overnight at 4°C and then with the secondary antibody for 1 h at room temperature. Immunolabeled cells were mounted in VECTASHIELD® antifade mounting media with or without DAPI (Vector Laboratories), then examined under a confocal microscope. Primary antibodies included mouse against GBA (Abcam) and mouse against HA (Sigma), and the secondary antibodies include the Alexa Fluor 568 and the 647 anti-mouse (Thermo Fisher Scientific).

Induction of Intracellular αS Inclusions by Exogenous αS Fibrils

H4/V1S:SV2/LAMP1-eCFP/mCherry-galectin-3 cells with GBA1 deletion (GBA1-) or without (WT) were treated with mature fibrils derived from recombinant αS fused with HA tag (αSHA)

as described previously (Jiang et al., 2008). Such αSHA fibrils were preincubated at 4°C for 2 days to facilitate the endocytosis seeding pathway because such incubation can significantly reduce the capability of αS fibrils in direct penetration of cell membrane according to our previous study (Jiang et al., 2017). Cells were fixed when GBA- cells formed enough seeded αS inclusions under confocal microscope. A portion of sibling cells from each group was subjected to immunocytochemical staining with antibody against HA tag to demonstrate the distribution of exogenous αSHA -fibrils (shown as Alexa Fluor™ 647). Another portion of cells was subjected to electron microscopy (EM) samples process and subsequent conventional EM and immunocytochemistry (EM). Immunocytochemistry was performed by immunolabeling Venus (orb334993, Biorbyt) and HA tag with a gold of 15 nm (25806, EMS) and 2 nm (25125, EMS) in samples, respectively.

Electron Microscopy and Immunoelectron Microscopy

Cells for transmission EM were fixed with 2% glutaraldehyde, 2% PFA in 0.1 M PBS; cells for Immunoelectron Microscopy (immunoEM) were fixed with 4% PFA in 0.1 M PBS. For EM, cells were postfixed in 1% OsO_4 ; washed three times in distilled water; stained with 1% uranyl acetate in 50% ethanol; and dehydrated with 70, 80, 95, and 100% ethanol sequentially. The cells were then treated with propylene oxide, infiltrated, and embedded in Epon 812 (Polysciences). For immunoEM, the cells were dehydrated in 30, 50, 70, and 90% ethanol, sequentially, then 90% ethanol-LR White (1:1) and 90% ethanol-LR White resin (1:2). They were then infiltrated and embedded in pure LR White. Ultrathin sections were cut from the Epon 812 or LR White-embedded samples by Leica Ultramicrotome. Ultrathin sections were examined after counterstaining with uranyl acetate and lead citrate. The sections were examined and photographed with a Philips 208S electron microscope.

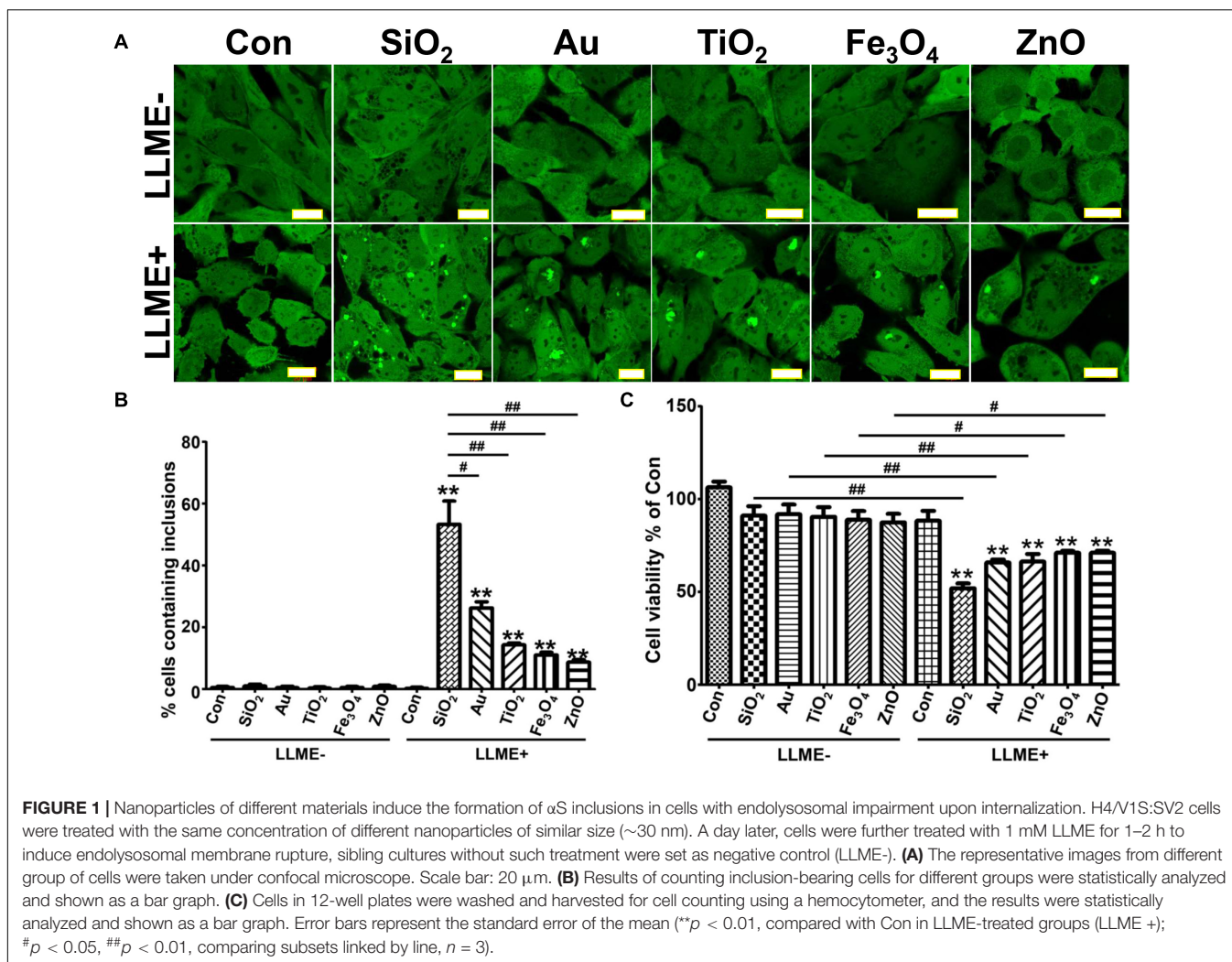
Statistical Analysis

Data from at least three sets of independent experiments were analyzed by one-way ANOVA with Dunnett's *post hoc* test or Student's *t*-test for the comparison of groups >3 and $(=2)$, respectively, to determine statistical significance.

RESULTS

Internalization of Different Nanoparticles With Similar Size Induces the Formation of αS Inclusions in a Cell Model With Endolysosomal Impairment

First, we want to know if nanoparticles from different materials are able to induce the formation of αS aggregates within cells. For this purpose, we tested nanoparticles that have been shown to promote αS to aggregate in salt solutions through direct interaction or to accumulate in cells through an indirect mechanism (Alvarez et al., 2013; Joshi et al., 2015; Xie and Wu, 2016; Mohammadi and Nikkhah, 2017; Tahaei Gilan et al., 2019; Khodabandeh et al., 2020). The nanoparticles tested were as follows: SiO_2 , Ti_2O_3 , Fe_2O_3 , and ZnO . To maximize the



comparability of results from different nanoparticles, only those with similar size (~30 nm) were used.

The cell model used for the evaluation of nanoparticle-induced α S aggregation was derived from H4 neuroglioma cell line (ATCC® HTB-148™). H4 cells were transfected to stably express the N-terminal half of Venus YFP tagged to α S (V1S) and C-terminal half of Venus YFP tagged to α S (SV2). This transfectant, referred to as H4/V1S:SV2, is useful for monitoring the aggregation of α S in live cells in real time. Because binding between V1S and SV2 will reconstitute YFP fluorescence, the brightness of fluorescence emitted can be used to estimate the extent of α S aggregation (Jiang et al., 2017). H4/V1S:SV2 cells growing in eight-well-chambered culture coverglass were treated with the same concentration of different nanoparticles (30–40 μ g/ml) and then observed under confocal microscope daily to monitor the formation of α S inclusions.

Our results showed no evidence of α S inclusions in cells after 1 week of nanoparticle treatment. Since using H4/V1S:SV2 cells to visualize α S aggregation induced by exogenous seeds is a well-established experiment in our laboratory (Jiang et al., 2017),

and the time for the induced α S inclusion to appear in this cell line has never been more than 3 days, we deduced that such negative results could be due to insufficient nanoparticles escaping the endocytic pathway to interact with cytoplasmic α S. If this is the case, cells with impaired endolysosomes should allow more nanoparticles to enter the cytoplasm. Since lysosomal dysfunction has been suggested to be an important pathogenic mechanism in PD (Dehay et al., 2010, 2012; Moors et al., 2016), we wondered if α S aggregation could be induced by nanoparticles in cells with endolysosomal impairment. For this purpose, the lysosomotropic detergent LLME that impairs endolysosomal function by irreversible accumulation in acidic compartments, leading to damage of endolysosomal membranes (Uchimoto et al., 1999) was chosen.

Cells treated with different nanoparticles for 1 day were exposed to 1 mM LLME to disrupt the integrity of endolysosomal membranes. As expected, after 1–2 h in LLME, all nanoparticle-treated cells developed α S inclusions. We observed differences in the ability of different nanoparticles to induce the formation of α S inclusions (Figures 1A,B). Moreover, nanoparticle-treated cultures exposed to LLME had fewer cells compared

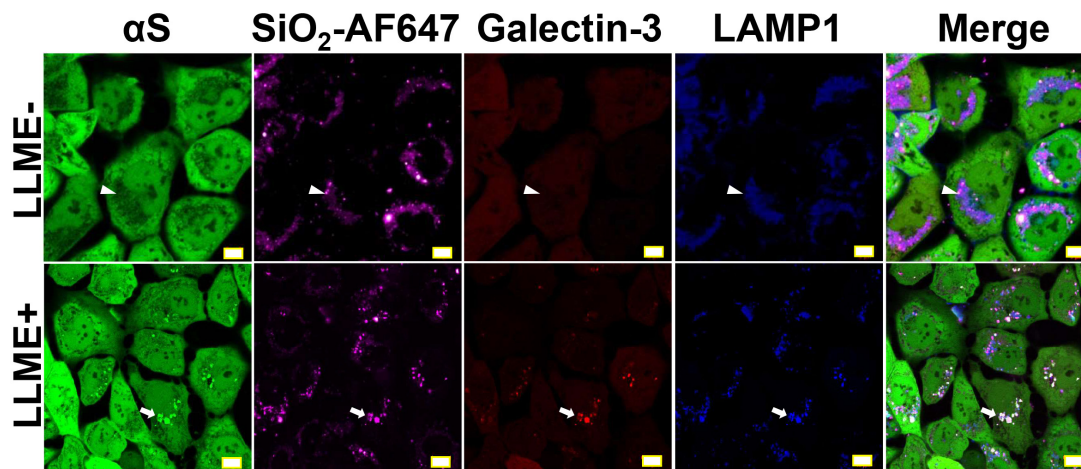


FIGURE 2 | Endolysosomal membrane rupture plays an essential role in the formation of nanoparticle-induced α S inclusions.

H4/V1S:SV2/LAMP1-eCFP/mCherry-galectin-3 cells were exposed to media supplemented with the same concentration of Alex FluorTM 647-labeled SiO₂ nanoparticles. A day later, cells were treated with 1 mM LLME to induce endolysosomal membrane rupture; sibling cultures without such treatment were set as negative control (LLME-). After 1–2 h, cells were subjected to imaging to show the distribution of intracellular nanoparticles (Alex FluorTM 647), α S inclusions (accumulated Venus), endolysosome (eCFP), and ruptured endolysosomes (punctuated mCherry-galectin-3), and their colocalization (denoted by white arrows and arrow-heads) under a confocal microscope. Scale bar: 10 μ m.

to those without such exposure, and the difference was statistically significant. Exposing cells to LLME in the absence of nanoparticles for 1–2 h did not result in either formation of α S inclusions or cell death, indicating that the nanoparticle-induced α S inclusions are cytotoxic (Figure 1C).

Next, we explored if nanoparticle-induced α S inclusions were associated with the rupture of endolysosomal membranes. For this study, we focused on SiO₂ nanoparticles, because cells treated with SiO₂ had the most α S inclusions (Figures 1A,B). Moreover, SiO₂ nanoparticles are less expensive, and they are the most common nanoparticle used in humans, such as in cosmetics (Napierska et al., 2010; Murugadoss et al., 2017).

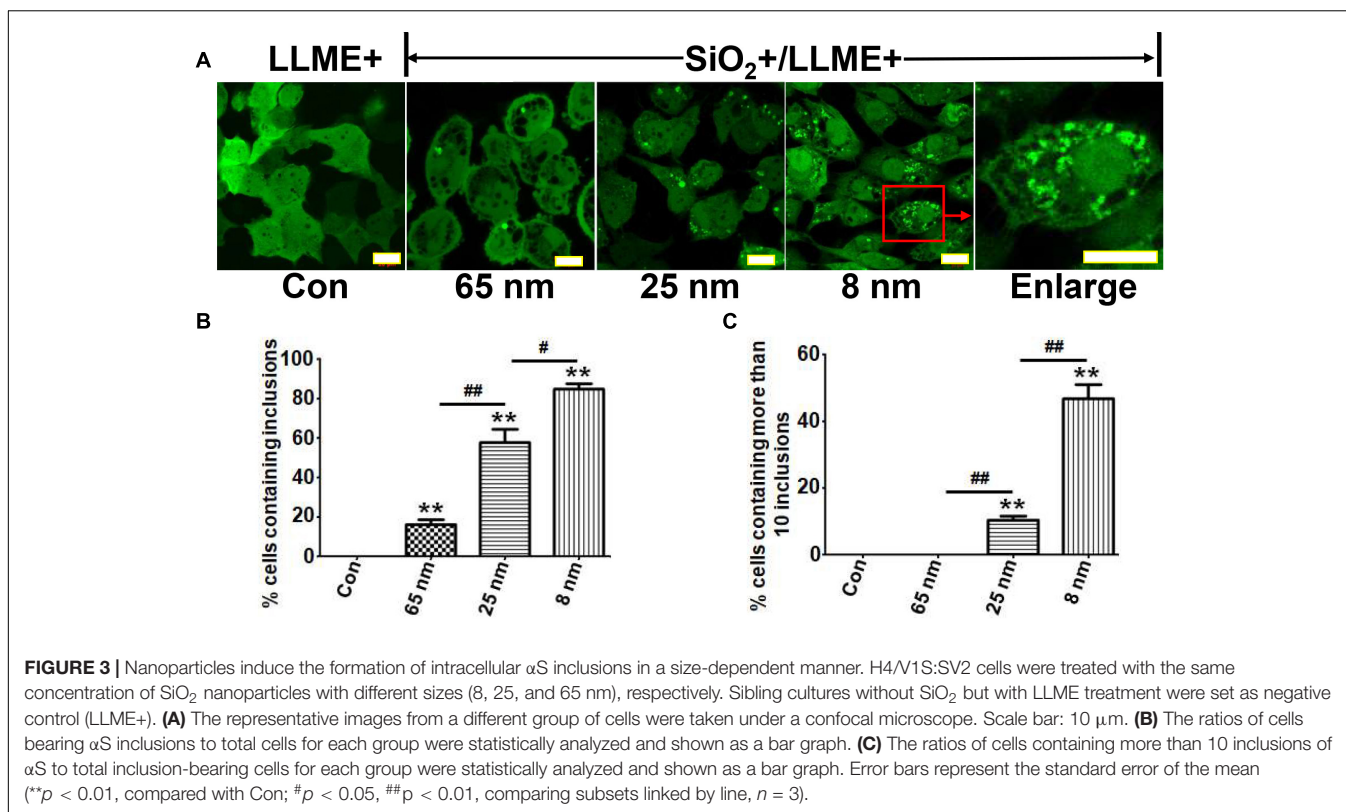
Endolysosomal Impairment Plays an Essential Role in the Formation of Nanoparticle-Induced α S Inclusions

Since the accumulation of galectin-3 on endolysosomal membrane is an indicator of endolysosomal rupture (Flavin et al., 2017), we introduced mCherry-tagged galectin-3 (mCherry-galectin-3) and eCFP-tagged LAMP1 (LAMP1-eCFP) into H4/V1S:SV2 cells to generate a new cell line referred to as H4/V1S:SV2/LAMP1-eCFP/mCherry-galectin-3. Cells from these transfectants were treated with Alex FluorTM 647-labeled SiO₂ nanoparticles (SiO₂-AF647) for 1 day, then exposed to LLME. Under confocal microscopy, we found that all induced α S inclusions were closely associated with galectin-3 and LAMP1 as reflected by the colocalization of Venus, mCherry, and eCFP (arrows in Figure 2). In contrast, cells treated with SiO₂ nanoparticles alone showed the retention of nanoparticles in endolysosomes, no rupture of endolysosomes, and no α S inclusions, as reflected by colocalization between Alex FluorTM 647 and eCFP without the accumulation of mCherry and Venus

(denoted by arrow heads in Figure 2). These results strongly supported that endolysosomal membrane rupture may play a role in nanoparticle-induced formation of α S inclusions.

Nanoparticles Induce the Formation of Intracellular α S Inclusions in a Size-Dependent Manner

It is known that the size of nanoparticles can highly influence their *in vivo* pharmacokinetics and cellular interaction (e.g., cellular uptake, biodistribution, and circulation half-life) (Hoshyar et al., 2016). Therefore, we studied the influence of nanoparticle size on the formation of α S inclusions. H4/V1S:SV2 cells were treated with SiO₂ nanoparticles of three different sizes (8, 25, and 65 nm), respectively, then exposed to LLME. For this experiment, the concentration of nanoparticles was 200 μ g/ml, which is over-saturated because nanoparticles of all three different sizes at lower concentration did not show a consistent proportion of α S inclusion-bearing cells. Using saturation levels of nanoparticles excludes the possibility that observed differences between different-sized nanoparticles were due to the presence of more small nanoparticle particles than large ones at a given concentration. Our results showed that the ratio of cells containing α S inclusions to total cells was about 16, 58, and 85%, respectively, for cells treated with nanoparticles of 65, 25, and 8 nm in size (Figures 3A,B). In addition, we found that in cultures treated with smaller nanoparticles, more cells contained multiple α S inclusions. The ratios of cells containing more than 10 inclusions of α S to total inclusion-bearing cells were 0, 13, and 55%, respectively, for those treated with nanoparticles of 65, 25, and 8 nm in size (Figures 3A,C). These results indicated that nanoparticles induce the formation of intracellular α S inclusions in a size-dependent manner.



Nanoparticles Induce α S to Form Detergent-Insoluble Aggregates Accompanied With an Increase in Pathological Form of α S

Next, we determined if nanoparticle-induced aggregates contain detergent-insoluble α S. Because H4/V1S:SV2 cells express a Venus tag-fused α S, to rule out the possible promotive effect of Venus on the formation of detergent-resistant α S, we used a cell line, 3D5 (Ko et al., 2008), expressing unlabeled α S. Cells of this model were derived from a neuroblastoma BE(2)-M17 cell line. They inducibly express wild-type human α S through a Tetoff mechanism and display neuronal phenotypes upon retinoic acid-induced differentiation (Ko et al., 2008). 3D5 cells were differentiated and induced to express α S in media with retinoic acid, but without Tet (see Figure 4A). On the 5th day, half of the cultures were treated with SiO_2 nanoparticles for 24 h. Subsequently, cultures with and without nanoparticle treatment were treated with LLME for 1–2 h. The other half served as control. The four groups of cells were referred to as Con (without any treatment), LLME (treated with LLME only), SiO_2 (treated with SiO_2 nanoparticles only), and SiO_2 /LLME (treated with both SiO_2 nanoparticles and LLME), respectively. They were harvested for protein extraction to separate Triton detergent (Tx)-soluble and insoluble fractions. Both fractions were then analyzed by SDS-PAGE and Western blotting for the detection of α S. The results showed that SiO_2 /LLME had the most α S oligomers in Tx-soluble fraction; and only SiO_2 /LLME contained α S aggregates in Tx-insoluble fractions (Figure 4C).

We further tested if phosphorylation on those α S aggregates occurs during the treatment. Results showed that the form of α S phosphorylated at serine 129 was also evidently increased in the group of SiO_2 /LLME in both fractions (Figure 4C). Therefore, in the presence of LLME, nanoparticles can induce our cell model to form detergent-insoluble α S aggregates, which is accompanied by an increase of pathological form of α S (phosphorylation at serine 129) (Bernal-Conde et al., 2019). Moreover, immunoblotting (Figure 4C) demonstrated the presence of higher cleaved Caspase 3 in SiO_2 /LLME than other samples, suggesting the formation of α S aggregates was associated with apoptotic cell death.

The Binding Affinity of Nanoparticles to α S Determines Its Capability to Induce α S Aggregation in Cells

Since previous studies have shown that the effects of nanoparticles on α S aggregation are associated with their mutual binding affinity (Alvarez et al., 2013; Mohammadi and Nikkha, 2017; Tahaei Gilan et al., 2019), we investigated if binding affinity plays a role in the formation of α S inclusions in cells after the internalization of nanoparticles. To answer this question, we designed an experiment that used nanoparticles with and without strong binding affinity to α S as positive and negative controls. Therefore, we compared the affinity to α S between nanoparticles from different materials and chose SiO_2 and chitin nanoparticles with similar size (80 nm) as the two controls because binding studies showed that there

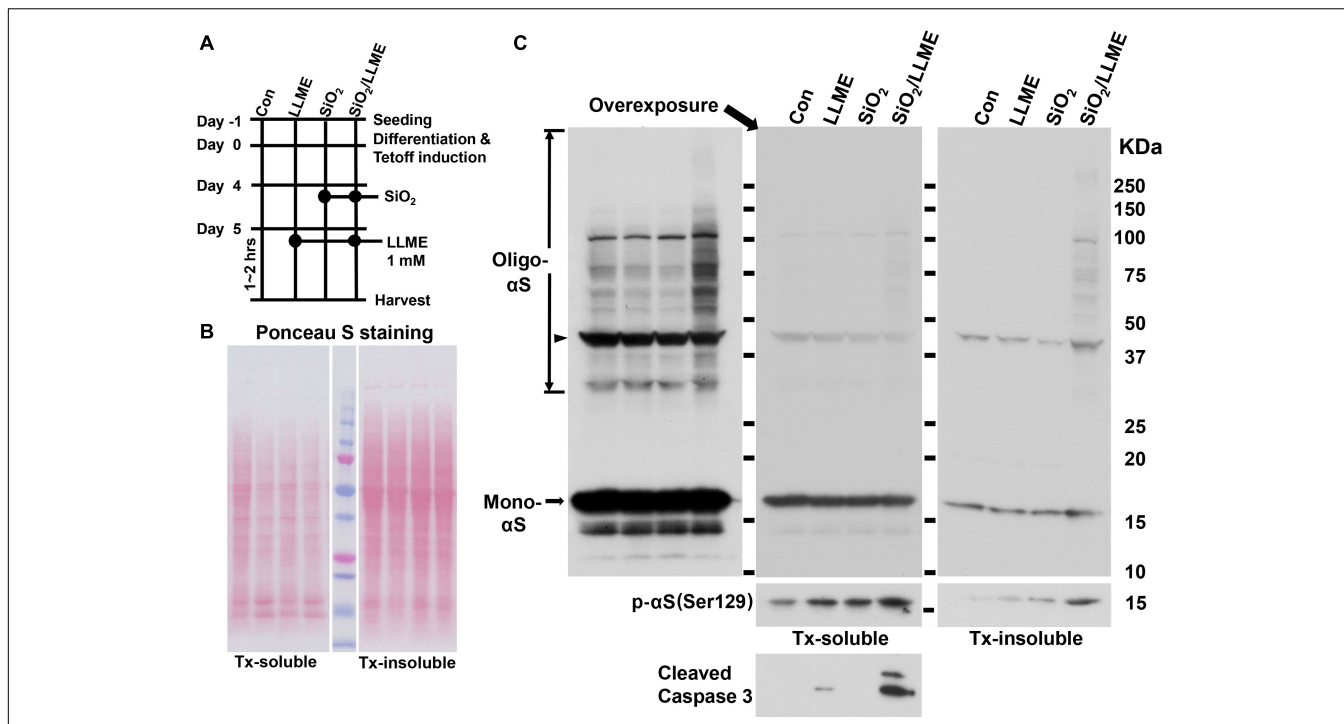


FIGURE 4 | Nanoparticles promote α S to form detergent-insoluble aggregates accompanied with an increase of pathological form of α S. **(A)** shows the experimental design. **(B)** Polyvinylidene difluoride (PVDF) membranes with transferred proteins were stained with Ponceau S to show that the amount of protein in different lanes was comparable. **(C)** After Ponceau S destaining and milk blocking, the blots were subjected to immunoblotting with antibodies against α S (610786, BD Biosciences), phosphorylated α S at serine 129 (pSyn #64, FUJIFILM Wako), and cleaved caspase 3 (9661, Cell Signaling), respectively. Monomeric and oligomeric α S were denoted by arrows; non-specific bands between 37 and 50 KDa were denoted by arrowhead.

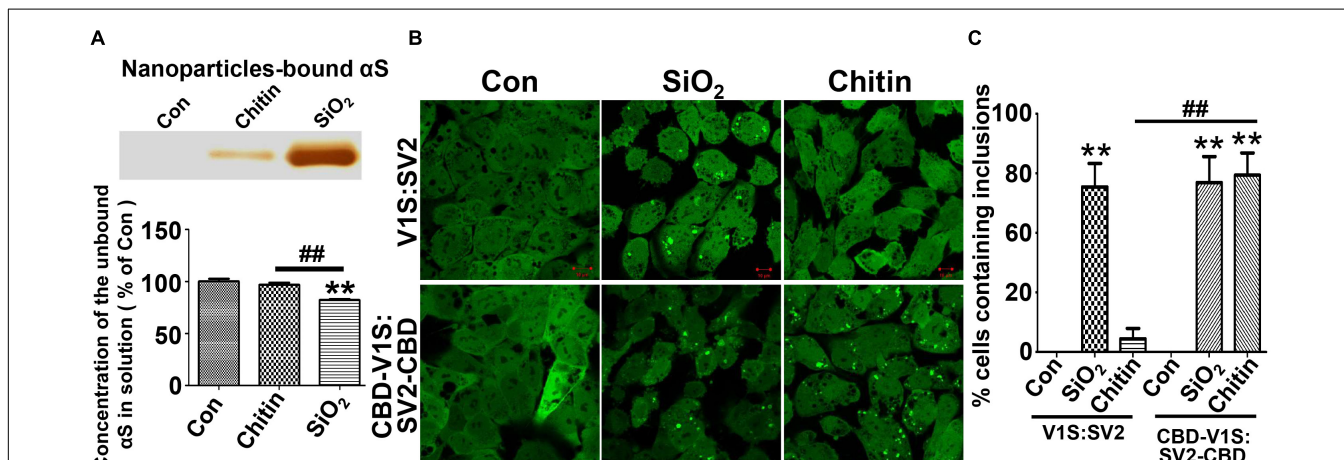
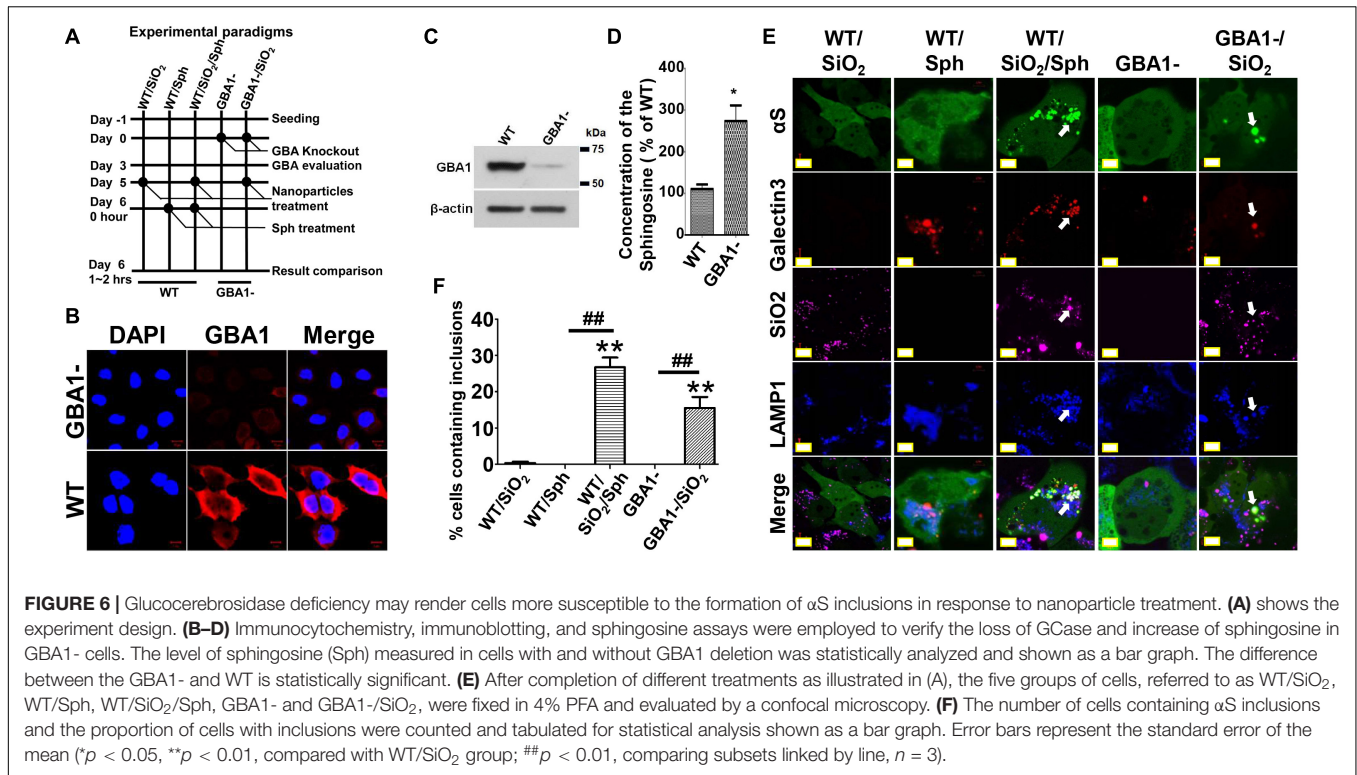


FIGURE 5 | The binding affinity of nanoparticles to α S determines its capability to induce the formation of α S inclusions. **(A)** Results of silver staining demonstrated that more α S was sequestered by SiO_2 than chitin nanoparticles (see the top panel); such sequestration occurred at the expense of soluble α S. The statistical analysis of unbound α S remained in nanoparticle-deprived solution was shown as a bar graph at the bottom panel. **(B)** The representative images were taken under a confocal microscope from “H4/CBD-V1S:SV2-CBD” and “H4/V1S:SV2” cells exposed to SiO_2 and chitin nanoparticles plus 1 mM LLME. **(C)** The ratios of cells containing α S inclusions to total cells for each group in B) are statistically analyzed and shown as a bar graph. Error bars represent the standard error of the mean (** $p < 0.01$, compared with Con group; ## $p < 0.01$, comparing subsets linked by line, $n = 3$).

was considerable α S bound to SiO_2 nanoparticles, while only negligible α S bound to chitin nanoparticles (Figure 5A).

Next, we establish a new cell line that stably co-expresses chitin binding domain (CBD)-tagged V1S at N-terminus (CBD-V1S)

and SV2 at C-terminus (SV2-CBD), referred to as “H4/CBD-V1S:SV2-CBD” (see Supplementary Figure 1). Due to the nature of CBD (Hashimoto et al., 2000), both CBD-V1S and SV2-CBD expressed in this cell line can specifically bind to exogenous chitin



nanoparticles. If binding affinity to α S is a determining factor for the induction of α S inclusions by nanoparticles, H4/CBD-V1S:SV2-CBD cells with endolysosomal impairment should form α S inclusions upon the treatment with chitin nanoparticles and LLME because CBD fused α S is able to specifically bind chitin through its CBD tag. In contrast, the number of α S inclusions induced by chitin nanoparticles in H4/V1S:SV2 cell line with lysosomal impairment should be significantly less because there is only negligible binding between α S and chitin due to the absence of CBD. However, SiO₂ nanoparticles should induce α S inclusions in both cell lines due to their significantly higher affinity to α S. Results from the cell-based study were exactly consistent with our expectations (see **Figures 5B,C**), strongly supporting the hypothesis that binding affinity of nanoparticles to α S determines their capability to induce α S inclusions in cells.

Lysosomal Glucocerebrosidase Deficiency May Render Cells More Susceptible to α S Inclusions in Response to Nanoparticle Treatment

The effect of LLME on endolysosomal impairment prompted us to study if there were endogenous lysosomotropic substances in human cells that are associated with PD. We found sphingosine to be a potential candidate. Sphingosine is an endogenous biomolecule significantly increased in patients with Gaucher disease (GD) due to the Glucocerebrosidase (GCase) deficiency in this disease (Mistry et al., 2014). It is also a lysosomotropic reagent similar to LLME as its accumulation in cells leads to the formation of dilated endolysosomes (Lima et al., 2017). GD is

the most common of the lysosomal storage diseases, and it is caused by a hereditary deficiency of the enzyme GCase, which is encoded by a gene named *GBA1*. Interestingly, mutation of *GBA1* gene recently emerged as a common genetic risk associated with PD. Approximately 5% of patients with PD carry a *GBA1* mutation, compared to <1% of the control population (Stoker et al., 2018). Moreover, a decrease in GCase activity has been detected in idiopathic brain tissue of PD (Chiasserini et al., 2015; Parnetti et al., 2017). Therefore, we hypothesized that GCase deficiency may render cells more susceptible to the formation of α S inclusions in response to nanoparticle treatment.

To test this hypothesis, cells with *GBA1* gene deletion were generated and used to assess α S aggregation in response to nanoparticles. As shown in **Figure 6A**, H4/V1S:SV2/LAMP1-eCFP/mCherry-galectin-3 cells were infected with lentivirus carrying *GBA1*-knockout and control vectors, referred to as “*GBA1*-” and “WT.” After 3 days of infection, a portion of sibling cells from WT and *GBA1*- were harvested to evaluate the effect of *GBA1* deletion on the level of GCase expression (**Figures 6B,C**) and sphingosine production (**Figure 6D**). A part of sibling cultures from “WT” and “*GBA1*-” groups were then treated with Alex Fluor™ 647-labeled SiO₂ nanoparticles to derive two subgroups, referred to as “WT/SiO₂” and “*GBA1*-/SiO₂.” After 1 day, “WT” cells with and without SiO₂ nanoparticle treatment were exposed to sphingosine (Sph, 20 μ M) to induce endolysosomal impairment, which further derived two more subgroups referred to as “WT/Sph” and “WT/SiO₂/Sph.” An hour after sphingosine exposure, cells in all groups were fixed with 4% PFA and evaluated by confocal microscopy for the presence of α S inclusions. As expected, Sph treatment

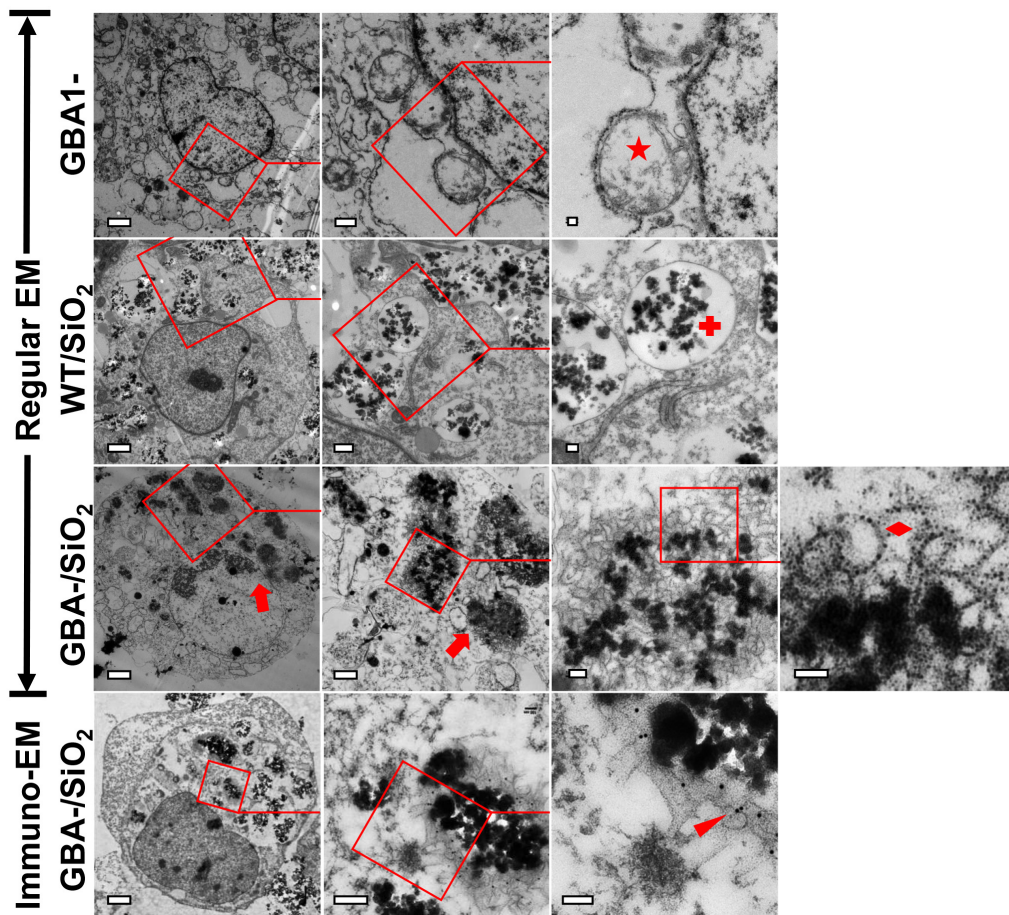


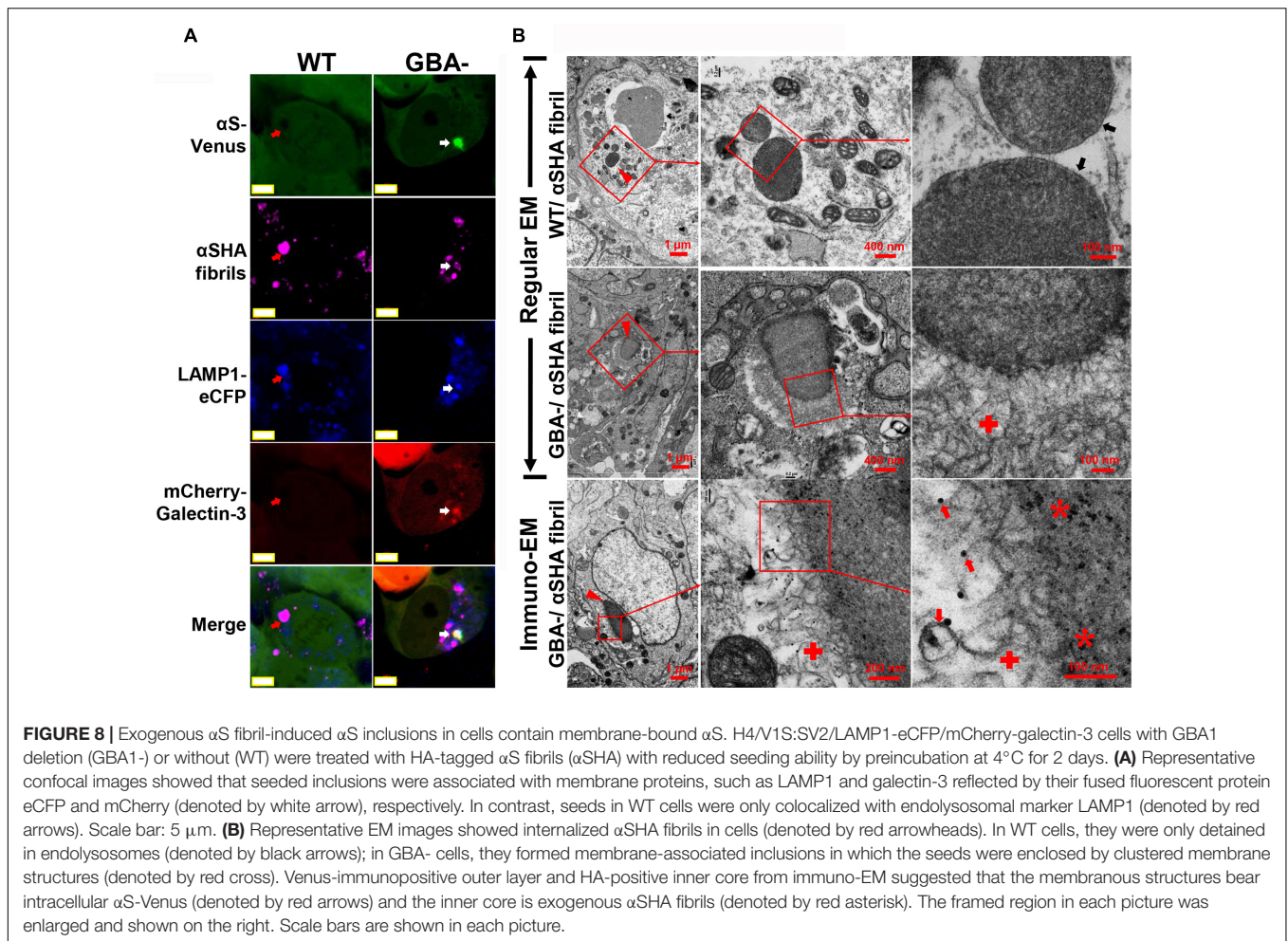
FIGURE 7 | Nanoparticle-induced α S inclusions contained membrane-bound α S. Three groups of cells, WT/SiO₂, GBA1-/SiO₂, and GBA1-, described in **Figure 6**, were prepared for EM examination. Uranyl-lead EM staining revealed that only cells in GBA1-/SiO₂ group contained abundant nanoparticle-associated inclusions (denoted by red arrows). The fields on the **left panels** were magnified in the **middle panels** and further in the **right panels** to reveal the presence of inclusions in the cells of GBA1-/SiO₂ group, and the inclusions contained a cluster of membranous structures in the absence of intact encircling membrane and filamentous structure (denoted by a red diamond), indicating that the endolysosomes in cells were ruptured and no α S fibril was formed. In contrast, cells in WT/SiO₂ group contained abundant congregated nanoparticles which were well-confined in intact endolysosomes (denoted by a red cross), and those in GBA1- group contain abundant abnormally swollen membranous structures (denoted by a red star). Immuno-EM further showed that the nanoparticle-associated membranous structures in GBA1-/SiO₂ group were immunolabeled by primary antibody against α S (NACP98, Mayo Clinic) (Dickson et al., 1999) and 18-nm gold conjugated secondary antibody (111-215-144, Jackson ImmunoResearch Laboratories) as denoted by a red arrowhead. Scale bar: 2 μ m for the first column; 500 nm for the second column; 100 nm for the third and fourth column.

or *GBA1* deletion both induced endolysosomal membrane rupture, reflected by colocalization of LAMP-eCFP and punctate mCherry-galectin-3 signals in cells. No α S inclusions were observed in cells with either endolysosomal rupture induction (GBA1- or WT/Sph) or nanoparticle treatment alone (WT/SiO₂). In contrast, cells with both nanoparticle treatment and endolysosomal impairment (WT/SiO₂/Sph and GBA1-/SiO₂) developed α S inclusions in numbers significantly different from the groups of WT/SiO₂, GBA1-, and WT/Sph (**Figures 6E,F**). Since cells with *GBA1* deletion had a significantly higher level of sphingosine (**Figure 6D**), and either *GBA1* deletion or exogenous sphingosine treatment can induce endolysosomal membrane rupture and facilitate nanoparticles to induce the formation of α S inclusions, it is reasonable to conclude that GCase deficiency may render cells more susceptible to the formation of α S inclusions

in response to nanoparticle treatment due to the high risk of impairment in endolysosomal system.

Nanoparticle-Induced Inclusions Contain Membrane-Bound α S

To understand the ultrastructure of nanoparticle-induced α S inclusions in cells with GCase deficiency, cultures belonging to the groups WT/SiO₂, GBA1-/SiO₂, and GBA1- were processed for EM examination. Our observations (**Figure 7**) revealed that only cells in GBA1-/SiO₂ group contained abundant nanoparticle-associated inclusions. In contrast, cells in WT/SiO₂ group contained abundant aggregated nanoparticles within endolysosomes (denoted by red cross in **Figure 7**), consistent with the view that nanoparticles are internalized *via* endocytosis



(Behzadi et al., 2017). Moreover, those in GBA1- group had abnormally swollen membranous structures (denoted by red star in Figure 7), similar to those observed in neurons from animals with *GBA1* knockout (Uemura et al., 2015; Schondorf et al., 2018). The inclusions detected in GBA1-/SiO₂ group consisted of a mixture of congregated nanoparticles and fragmented membranous structures in the absence of intact encircling membrane and filamentous structure (denoted by red diamond in Figure 7), indicating that the endolysosomes in cells were ruptured and no α S fibril was formed.

Subsequent immuno-EM staining revealed that the nanoparticle-associated membranous structures were immunoreactive to antibody against α S (denoted by red arrowhead in Figure 7), suggesting that the membrane-bound α S is a constituent of the nanoparticle-induced inclusion.

Exogenous α S Fibril-Induced α S Inclusions in Cells Contain Membrane-Bound α S

As we know, α S fibrils can recruit unfolded α S to amplify aggregates in buffer system; moreover, exogenous α S fibrils can seed the formation of Lewy body-like intracellular inclusions in

cultured cells (Luk et al., 2009). If membrane-bound α S is a constituent of nanoparticle-induced α S inclusions, it should also exist in α S fibril-induced inclusions due to the mutual affinity between α S fibrils and α S molecules. To find the answer, we used mature fibrils derived from recombinant α S fused with HA tag (α SHA) to treat H4/V1S:SV2/LAMP1-eCFP/mCherry-galectin-3 cells with GBA1 deletion (GBA1-) or without (WT). Cells of GBA1- should be more susceptible to the formation of α S inclusions due to the endolysosomal impairment compared with those of WT. Results from confocal imaging showed that seeded inclusions were associated with membrane proteins, such as LAMP1 and galectin-3 reflected by their fused fluorescent protein eCFP and mCherry (in Figure 8A), respectively, suggesting the involvement of membrane structures and membrane rupture in seeding. In contrast, seeds in WT cells were only colocalized with endolysosomal marker LAMP1, suggesting its endocytic pathway of cellular uptake, but did not induce α S inclusion due to the confinement of nanoparticles in endolysosomes. Results from EM showed that α SHA fibrils were internalized by cells. In WT cells, they were only detained in endolysosomes; In GBA- cells, they formed membrane-associated inclusions in which the seeds were enclosed by clustered membrane structures. Moreover, immuno-EM revealed that the inclusions consisted

of Venus-immunopositive membranous outer layer and HA-immunopositive inner core (denoted by red asterisk), suggesting that these inclusions were formed by the seeding between exogenous α SHA fibrils and cytoplasmic membrane-bound α -Venus.

DISCUSSION

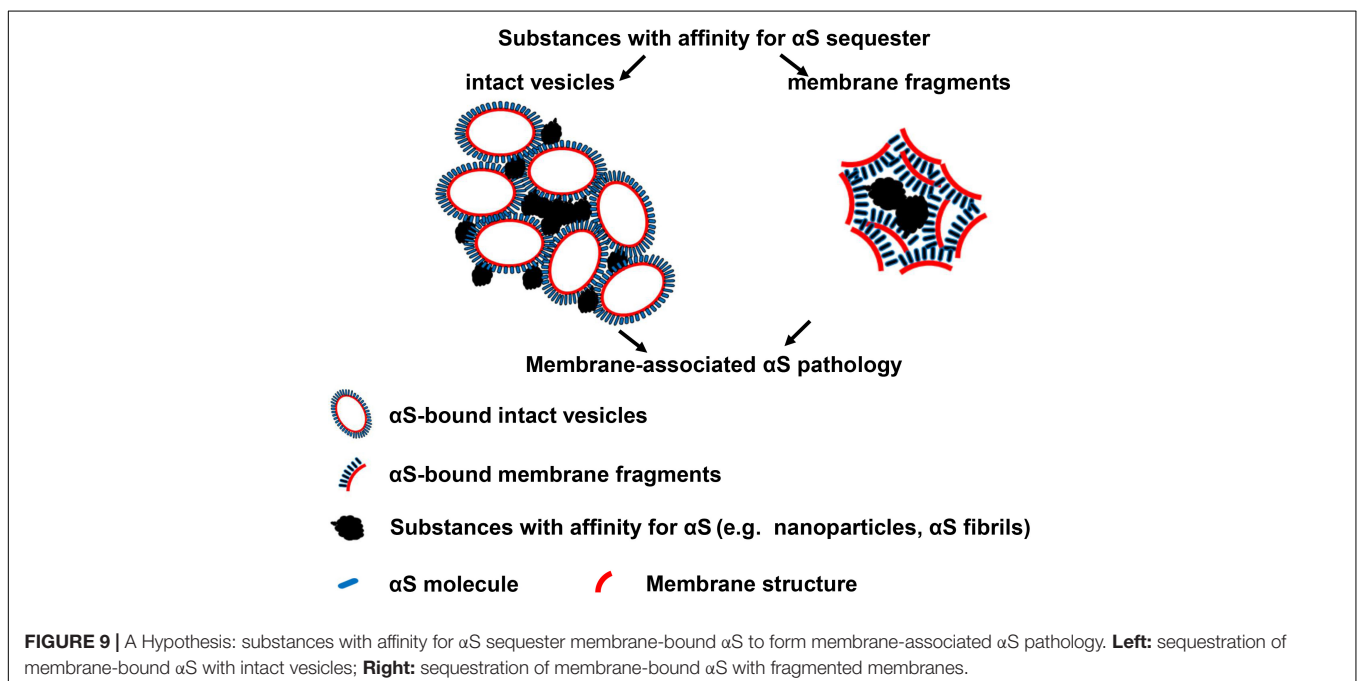
Although over recent decades nanoparticle-based therapies have been explored as a potential tool for disease treatment, it still remains controversial if such strategy is applicable to the treatment of neurodegenerative diseases (Mushtaq et al., 2015; Naqvi et al., 2020). As we know, the accumulation of aggregated protein is a prominent feature of neurodegenerative diseases, and the aggregate-prone proteins, which are highly expressed in brain cells, could be sequestered by nanoparticles if there is mutual affinity. This brings up a question as to whether the accumulated proteins on the surface of nanoparticles could aggregate and become toxic. As for α S, the major causative protein in PD, ample evidence from studies in buffer system has shown that the promotive or inhibitive effects of nanoparticles on this protein are determined by multiple factors, such as shape, surface charge, and concentration (D'Onofrio et al., 2020; Pichla et al., 2020). However, there were only limited studies focusing on the effect of nanoparticles on α S aggregation in cellular and animal models.

In the present study, we demonstrated that nanoparticles can induce α S assembly to form inclusions upon internalization into cells with endolysosomal impairment. It is worth noting that in cell treatment, only a portion of nanoparticles can successfully enter into cells and then escape from endolysosome to interact with cytoplasmic α S; therefore, nanoparticles at low concentration might not result in the best effect. However,

nanoparticles at too high concentration should also be avoided because cells overwhelmed by nanoparticles may become unhealthy. This is very different from experiments in a buffer system in which the concentration of nanoparticles for the induction of α S aggregation can be used in a wide range (Vitali et al., 2018; Pang et al., 2021). Therefore, the concentration of nanoparticles should be carefully optimized for cell treatment.

Although a previous study by Xie and Wu (2016) showed that SiO₂ nanoparticles can induce α S aggregates in PC12 cells, our study is the first report showing that nanoparticles can escape from ruptured endolysosomes (reflected by LAMP1-associated punctate galectin-3) to directly interact with cytoplasmic α S, leading to the formation of α S inclusions in cells with the impaired endolysosomal system. In the study by Xie and Wu (2016) nanoparticles were confined in endolysosomes and consequently not associated with detergent-insoluble α S, but there was an increase in α S levels in cells treated with nanoparticles compared with those without. They hypothesized that this was due to nanoparticle-elicited oxidative stress and inhibition of the ubiquitin-proteasomal system. To our knowledge, the present study is the first to show that nanoparticles may directly interact with cytoplasmic α S to form toxic aggregates.

Even though nanoparticle-induced α S inclusions in our cell models contained detergent-resistant and pathologic forms of α S aggregates, no filamentous α S structures were observed with immunoEM (Figures 4, 7). Therefore, the α S inclusions in our cell models should be formed at an early stage of α S aggregation. The formation of filamentous structures may require a longer duration of treatment, higher levels of α S expression, or other unknown cellular factors. It is unclear how α S aggregates upon contact with nanoparticles. A mechanism previously proposed for the aggregation of membrane-bound



α S may provide a reasonable explanation (Galvagnion et al., 2015). In that model, α S molecules normally bind and accumulate on membrane surfaces leading to locally high concentrations. Localized high concentration of α S may promote conformational changes that favor nucleation, which triggers a cascade of events leading to high molecular weight aggregates. If nanoparticles can bind α S, it might be predicted that they may sequester α S on the nanoparticle surface, which can favor nucleation and subsequent aggregation once a critical concentration is reached. This hypothesis was supported by experiments in which chitin nanoparticles induced the formation of α S inclusions in cells of “H4/CBD-V1S:SV2-CBD” due to sequestration of CBD-fused α S *via* the specific binding affinity between chitin and CBD tag. In contrast, “H4/V1S:SV2” cells lacking the CBD, the binding partner of chitin, did not lead to aggregation (Figure 5). Therefore, it is reasonable to suggest that exogenous or endogenous substances with binding affinity for α S, once in contact with cytoplasmic α S, may promote α S pathology in humans.

We found that endolysosomal impairment is critical in the susceptibility of cells to nanoparticle-induced formation of α S inclusions. This is supported by the fact that cultured cells can develop nanoparticle-induced α S inclusions only if their endolysosomal system is disrupted by treatment with lysosomotropic agents or GCase deficiency (Figures 2, 6). In this regard, we further demonstrated that sphingosine, an endogenous lysosomotropic biomolecule, plays an important role in determining the susceptibility of cells to α S inclusions in the presence of nanoparticles. In these cells, increased sphingosine levels due to *GBA1* deletion or GCase deficiency impair endolysosomal integrity (Figures 6, 7). It is worth noting that GCase deficiency is associated with the accumulation of multiple lipid metabolites (Abed Rabbo et al., 2021), and sphingosine may not be the only critical factor in this process.

In addition, we found that smaller-sized nanoparticles were more effective in inducing the formation of α S inclusions (Figure 3). Size-dependent phenomenon may be related to the possibility that smaller nanoparticles more readily escape from endolysosomes. Alternatively, nanoparticles of smaller size have higher curvature on surface, which is more likely to promote protein aggregation, as shown in previous studies on the impact of membrane curvature on amyloid aggregation (Terakawa et al., 2018). Given these observations, caution needs to be taken when using nanoparticles in the treatment of PD, since lysosomal impairment has been considered to play an important role in PD and related diseases (Wang et al., 2018). Moreover, for the selection of nanoparticles, the size, the nature of material, and the binding affinity to α S on the surface should also be considered.

It is interesting that nanoparticle-induced α S inclusions contain a cluster of membranous structures at the ultrastructural level. This result is consistent with the finding reported by Shahmoradian et al. (2019) that Lewy pathology in PD consists of crowded lipid membranes. More importantly, such membranous structures can be immunolabeled by antibody against α S, indicative of membrane-bound α S (Figure 7). This result suggests a role of membranous structures in the formation of α S pathology because membrane-bound α S has a higher propensity

for aggregation into higher-order oligomers/aggregates (Lee et al., 2002; Burre et al., 2014). Although Shahmoradian et al. hypothesized that “lipid membrane fragments and distorted organelles together with a non-fibrillar form of α S are the main structural building blocks for the formation of Lewy pathology” (Shahmoradian et al., 2019), our results raised another possibility that a certain type of membranous structures, due to bearing high concentration of bound α S, may be recruited as byproducts by α S-affinitive substance (e.g., SiO₂ nanoparticles in the present study) to become an important constituent of α S pathology. If this is the case, the crowded lipid membranous structures observed in α S pathology in the brain, which has been considered mainly due to impaired organellar trafficking in previous studies (Hunn et al., 2015; Shahmoradian et al., 2019), could also result from sequestration of α S by substances with strong binding affinity to α S. Since unfolded α S can be recruited and templated by α S fibrils leading to the propagation of α S aggregates (Wood et al., 1999), it is reasonable to consider α S fibrils as a type of substances with strong binding affinity to α S. Accordingly, α S inclusions induced by α S fibrils should also contain α S-associated membranes. Indeed, this speculation was confirmed by our cell-based study. As shown in Figure 8, cells with *GBA1* deletion and α S fibrils treatment can form α S inclusions associated with membrane proteins, such as LAMP1 and galectin-3, and these inclusions also contained clustered membranous structures and membrane-bound α S at the ultrastructural level. Based on these results, we proposed that sequestration of membrane-bound α S by substances with binding affinity for α S (e.g., nanoparticles, α S filaments) could contribute to the formation of membrane-associated α S pathology. A schematic picture of this hypothesis is shown in Figure 9.

Overall, this study investigated the effect of nanoparticles with affinity for α S on α S aggregation in different cell models and made the novel observation that loss of endolysosomal integrity and the intrinsic binding affinity of the nanoparticles induced the sequestration of cytoplasmic α S. Furthermore, we propose a new mechanism to explain the role of crowded lipid membranous structures in Lewy pathology. This study not only provides support for the potential risk of nanoparticles in the treatment of neurologic disorders, especially for neurodegenerative diseases, such as PD and multiple system atrophy, which are associated with aggregation-prone α S, but it also advances understanding about mechanisms underlying the formation of α S pathology in PD.

DATA AVAILABILITY STATEMENT

The original contributions presented in the study are included in the article/Supplementary Material, further inquiries can be directed to the corresponding authors.

AUTHOR CONTRIBUTIONS

PJ created the ideas, designed and conducted the experiments, and wrote the manuscript. MG performed the data analysis and

image labeling. S-HY and DD revised the manuscript. All authors contributed to the article and approved the submitted version.

FUNDING

This study was supported by the National Institute of Health (U54 NS110435, UG3 NS104095, and R21 NS099757) and the

Mangurian Foundation Lewy Body Dementia Program at Mayo Clinic (DD and PJ).

SUPPLEMENTARY MATERIAL

The Supplementary Material for this article can be found online at: <https://www.frontiersin.org/articles/10.3389/fnmol.2021.738535/full#supplementary-material>

REFERENCES

- Abed Rabbo, M., Khodour, Y., Kaguni, L. S., and Stiban, J. (2021). Sphingolipid lysosomal storage diseases: from bench to bedside. *Lipids Health Dis.* 20:44. doi: 10.1186/s12944-021-01466-0
- Alvarez, Y. D., Fauerbach, J. A., Pellegrotti, J. V., Jovin, T. M., Jares-Erijman, E. A., and Stefani, F. D. (2013). Influence of gold nanoparticles on the kinetics of alpha-synuclein aggregation. *Nano Lett.* 13, 6156–6163. doi: 10.1021/nl403490e
- Bae, E. J., Yang, N. Y., Lee, C., Lee, H. J., Kim, S., Sardi, S. P., et al. (2015). Loss of glucocerebrosidase 1 activity causes lysosomal dysfunction and alpha-synuclein aggregation. *Exp. Mol. Med.* 47:e153. doi: 10.1038/emmm.2014.128
- Behzadi, S., Serpooshan, V., Tao, W., Hamaly, M. A., Alkawarek, M. Y., Dreaden, E. C., et al. (2017). Cellular uptake of nanoparticles: journey inside the cell. *Chem. Soc. Rev.* 46, 4218–4244. doi: 10.1039/C6CS00636A
- Bernal-Conde, L. D., Ramos-Acevedo, R., Reyes-Hernandez, M. A., Balbuena-Olvera, A. J., Morales-Moreno, I. D., Arguero-Sanchez, R., et al. (2019). Alpha-synuclein physiology and pathology: a perspective on cellular structures and organelles. *Front. Neurosci.* 13:1399. doi: 10.3389/fnins.2019.01399
- Burre, J., Sharma, M., and Sudhof, T. C. (2014). alpha-Synuclein assembles into higher-order multimers upon membrane binding to promote SNARE complex formation. *Proc. Natl. Acad. Sci. U.S.A.* 111, E4274–E4283. doi: 10.1073/pnas.1416598111
- Chiasserini, D., Paciotti, S., Eusebi, P., Persichetti, E., Tasegian, A., Kurzawa-Akanbi, M., et al. (2015). Selective loss of glucocerebrosidase activity in sporadic Parkinson's disease and dementia with Lewy bodies. *Mol. Neurodegener.* 10:15. doi: 10.1186/s13024-015-0010-2
- Dehay, B., Bove, J., Rodriguez-Muela, N., Perier, C., Recasens, A., Boya, P., et al. (2010). Pathogenic lysosomal depletion in Parkinson's disease. *J. Neurosci.* 30, 12535–12544. doi: 10.1523/JNEUROSCI.1920-10.2010
- Dehay, B., Martinez-Vicente, M., Ramirez, A., Perier, C., Klein, C., Vila, M., et al. (2012). Lysosomal dysfunction in Parkinson disease: ATP13A2 gets into the groove. *Autophagy* 8, 1389–1391. doi: 10.4161/auto.21011
- Dickson, D. W., Liu, W., Hardy, J., Farrer, M., Mehta, N., Uitti, R., et al. (1999). Widespread alterations of alpha-synuclein in multiple system atrophy. *Am. J. Pathol.* 155, 1241–1251. doi: 10.1016/S0002-9440(10)65226-1
- D'Onofrio, M., Munari, F., and Assfalg, M. (2020). Alpha-synuclein-nanoparticle interactions: understanding, controlling and exploiting conformational plasticity. *Molecules* 25:5625. doi: 10.3390/molecules25235625
- Flavin, W. P., Bousset, L., Green, Z. C., Chu, Y., Skarpathiotis, S., Chaney, M. J., et al. (2017). Endocytic vesicle rupture is a conserved mechanism of cellular invasion by amyloid proteins. *Acta Neuropathol.* 134, 629–653. doi: 10.1007/s00401-017-1722-x
- Galvagnion, C., Buell, A. K., Meisl, G., Michaels, T. C., Vendruscolo, M., Knowles, T. P., et al. (2015). Lipid vesicles trigger alpha-synuclein aggregation by stimulating primary nucleation. *Nat. Chem. Biol.* 11, 229–234. doi: 10.1038/nchembio.1750
- Gavhane, Y. N., and Yadav, A. V. (2012). Loss of orally administered drugs in GI tract. *Saudi Pharm. J.* 20, 331–344. doi: 10.1016/j.jsps.2012.03.005
- Hashimoto, M., Ikegami, T., Seino, S., Ohuchi, N., Fukada, H., Sugiyama, J., et al. (2000). Expression and characterization of the chitin-binding domain of chitinase A1 from *Bacillus circulans* WL-12. *J. Bacteriol.* 182, 3045–3054. doi: 10.1128/JB.182.11.3045-3054.2000
- Hata, K., Higashisaka, K., Nagano, K., Mukai, Y., Kamada, H., Tsunoda, S., et al. (2014). Evaluation of silica nanoparticle binding to major human blood proteins. *Nanoscale Res. Lett.* 9:2493. doi: 10.1186/1556-276X-9-668
- Hersh, D. S., Wadajkar, A. S., Roberts, N., Perez, J. G., Connolly, N. P., Frenkel, V., et al. (2016). Evolving drug delivery strategies to overcome the blood brain barrier. *Curr. Pharm. Des.* 22, 1177–1193. doi: 10.2174/1381612822666151221150733
- Hoshyar, N., Gray, S., Han, H., and Bao, G. (2016). The effect of nanoparticle size on in vivo pharmacokinetics and cellular interaction. *Nanomedicine* 11, 673–692. doi: 10.2217/nnm.16.5
- Hunn, B. H., Cragg, S. J., Bolam, J. P., Spillantini, M. G., and Wade-Martins, R. (2015). Impaired intracellular trafficking defines early Parkinson's disease. *Trends Neurosci.* 38, 178–188. doi: 10.1016/j.tins.2014.12.009
- Jiang, P., Gan, M., Ebrahim, A. S., Castanedes-Casey, M., Dickson, D. W., and Yen, S. H. (2013). Adenosine monophosphate-activated protein kinase overactivation leads to accumulation of alpha-synuclein oligomers and decrease of neurites. *Neurobiol. Aging* 34, 1504–1515. doi: 10.1016/j.neurobiolaging.2012.11.001
- Jiang, P., Gan, M., Yen, S. H., McLean, P. J., and Dickson, D. W. (2017). Impaired endo-lysosomal membrane integrity accelerates the seeding progression of alpha-synuclein aggregates. *Sci. Rep.* 7:7690. doi: 10.1038/s41598-017-08149-w
- Jiang, P., Ko, L. W., Jansen, K. R., Golde, T. E., and Yen, S. H. (2008). Using leucine zipper to facilitate alpha-synuclein assembly. *FASEB J.* 22, 3165–3174. doi: 10.1096/fj.08.108365
- Joshi, N., Basak, S., Kundu, S., De, G., Mukhopadhyay, A., and Chattopadhyay, K. (2015). Attenuation of the early events of alpha-synuclein aggregation: a fluorescence correlation spectroscopy and laser scanning microscopy study in the presence of surface-coated Fe3O4 nanoparticles. *Langmuir* 31, 1469–1478. doi: 10.1021/la503749e
- Khodabandeh, A. Y., Yakhchian, R., Hasan, A., Paray, B. A., Shahi, F., Rasti, B., et al. (2020). Silybin as a potent inhibitor of alpha-synuclein aggregation and associated cytotoxicity against neuroblastoma cells induced by zinc oxide nanoparticles. *J. Mol. Liquids* 310:113198. doi: 10.1016/j.molliq.2020.113198
- Ko, L. W., Ko, H. H., Lin, W. L., Kulathingal, J. G., and Yen, S. H. (2008). Aggregates assembled from overexpression of wild-type alpha-synuclein are not toxic to human neuronal cells. *J. Neuropathol. Exp. Neurol.* 67, 1084–1096. doi: 10.1097/NEN.0b013e31818c3618
- Lafuente, J. V., Requejo, C., and Ugedo, L. (2019). Nanodelivery of therapeutic agents in Parkinson's disease. *Prog. Brain Res.* 245, 263–279. doi: 10.1016/bs.pbr.2019.03.004
- Lee, H. J., Choi, C., and Lee, S. J. (2002). Membrane-bound alpha-synuclein has a high aggregation propensity and the ability to seed the aggregation of the cytosolic form. *J. Biol. Chem.* 277, 671–678. doi: 10.1074/jbc.M107045200
- Leyva-Gomez, G., Cortes, H., Magana, J. J., Leyva-Garcia, N., Quintanar-Guerrero, D., and Floran, B. (2015). Nanoparticle technology for treatment of Parkinson's disease: the role of surface phenomena in reaching the brain. *Drug Discov. Today* 20, 824–837. doi: 10.1016/j.drudis.2015.02.009
- Lima, S., Milstien, S., and Spiegel, S. (2017). Sphingosine and Sphingosine Kinase 1 Involvement in Endocytic Membrane Trafficking. *J. Biol. Chem.* 292, 3074–3088. doi: 10.1074/jbc.M116.762377
- Linse, S., Cabaleiro-Lago, C., Xue, W. F., Lynch, I., Lindman, S., Thulin, E., et al. (2007). Nucleation of protein fibrillation by nanoparticles. *Proc. Natl. Acad. Sci. U.S.A.* 104, 8691–8696. doi: 10.1073/pnas.0701250104
- Luk, K. C., Song, C., O'Brien, P., Stieber, A., Branch, J. R., Brunden, K. R., et al. (2009). Exogenous alpha-synuclein fibrils seed the formation of Lewy body-like intracellular inclusions in cultured cells. *Proc. Natl. Acad. Sci. U.S.A.* 106, 20051–20056. doi: 10.1073/pnas.0908005106

- Mahapatro, A., and Singh, D. K. (2011). Biodegradable nanoparticles are excellent vehicle for site directed in-vivo delivery of drugs and vaccines. *J. Nanobiotechnol.* 9:55. doi: 10.1186/1477-3155-9-55
- Meissner, W. G., Frasier, M., Gasser, T., Goetz, C. G., Lozano, A., Piccini, P., et al. (2011). Priorities in Parkinson's disease research. *Nat. Rev. Drug Discov.* 10, 377–393. doi: 10.1038/nrd3430
- Mhyre, T. R., Boyd, J. T., Hamill, R. W., and Maguire-Zeiss, K. A. (2012). Parkinson's disease. *Subcell. Biochem.* 65, 389–455. doi: 10.1007/978-94-007-5416-4_16
- Mistry, P. K., Liu, J., Sun, L., Chuang, W. L., Yuen, T., Yang, R., et al. (2014). Glucocerebrosidase 2 gene deletion rescues type 1 Gaucher disease. *Proc. Natl. Acad. Sci. U.S.A.* 111, 4934–4939. doi: 10.1073/pnas.1400768111
- Mohammadi, S., and Nikkhal, M. (2017). TiO₂ nanoparticles as potential promoting agents of fibrillation of alpha-Synuclein, a Parkinson's Disease-Related Protein. *Iran. J. Biotechnol.* 15, 87–94. doi: 10.15171/ijb.1519
- Moors, T., Paciotti, S., Chiasserini, D., Calabresi, P., Parnetti, L., Beccari, T., et al. (2016). Lysosomal dysfunction and alpha-synuclein aggregation in Parkinson's disease: diagnostic links. *Mov. Disord.* 31, 791–801. doi: 10.1002/mds.26562
- Murthy, S. K. (2007). Nanoparticles in modern medicine: state of the art and future challenges. *Int. J. Nanomed.* 2, 129–141.
- Murugadoss, S., Lison, D., Godderis, L., Van Den Brule, S., Mast, J., Brassinne, F., et al. (2017). Toxicology of silica nanoparticles: an update. *Arch. Toxicol.* 91, 2967–3010. doi: 10.1007/s00204-017-1993-y
- Mushtaq, G., Khan, J. A., Joseph, E., and Kamal, M. A. (2015). Nanoparticles, neurotoxicity and neurodegenerative diseases. *Curr. Drug Metab.* 16, 676–684. doi: 10.2174/1389200216666150812122302
- Napierska, D., Thomassen, L. C., Lison, D., Martens, J. A., and Hoet, P. H. (2010). The nanosilica hazard: another variable entity. *Part. Fibre Toxicol.* 7:39. doi: 10.1186/1743-8977-7-39
- Naqvi, S., Panghal, A., and Flora, S. J. S. (2020). Nanotechnology: a promising approach for delivery of neuroprotective drugs. *Front. Neurosci.* 14:494. doi: 10.3389/fnins.2020.00494
- Pang, C., Zhang, N., and Falahati, M. (2021). Acceleration of alpha-synuclein fibril formation and associated cytotoxicity stimulated by silica nanoparticles as a model of neurodegenerative diseases. *Int. J. Biol. Macromol.* 169, 532–540. doi: 10.1016/j.ijbiomac.2020.12.130
- Parnetti, L., Paciotti, S., Eusebi, P., Dardis, A., Zampieri, S., Chiasserini, D., et al. (2017). Cerebrospinal fluid beta-glucocerebrosidase activity is reduced in Parkinson's disease patients. *Mov. Disord.* 32, 1423–1431. doi: 10.1002/mds.27136
- Pichla, M., Bartosz, G., and Sadowska-Bartos, I. (2020). The antiaggregative and antiamyloidogenic properties of nanoparticles: a promising tool for the treatment and diagnostics of neurodegenerative diseases. *Oxid. Med. Cell. Longev.* 2020:3534570. doi: 10.1155/2020/3534570
- Raza, C., Anjum, R., and Shakeel, N. U. A. (2019). Parkinson's disease: mechanisms, translational models and management strategies. *Life Sci.* 226, 77–90. doi: 10.1016/j.lfs.2019.03.057
- Schondorf, D. C., Ivanyuk, D., Baden, P., Sanchez-Martinez, A., De Cicco, S., Yu, C., et al. (2018). The NAD⁺ precursor nicotinamide riboside rescues mitochondrial defects and neuronal loss in iPSC and fly models of Parkinson's Disease. *Cell Rep.* 23, 2976–2988. doi: 10.1016/j.celrep.2018.05.009
- Shahmoradian, S. H., Lewis, A. J., Genoud, C., Hench, J., Moors, T. E., Navarro, P. P., et al. (2019). Lewy pathology in Parkinson's disease consists of crowded organelles and lipid membranes. *Nat. Neurosci.* 22, 1099–1109. doi: 10.1038/s41593-019-0423-2
- Shang, L., Nienhaus, K., and Nienhaus, G. U. (2014). Engineered nanoparticles interacting with cells: size matters. *J. Nanobiotechnol.* 12:5. doi: 10.1186/1477-3155-12-5
- Shen, S., Wu, Y., Liu, Y., and Wu, D. (2017). High drug-loading nanomedicines: progress, current status, and prospects. *Int. J. Nanomed.* 12, 4085–4109. doi: 10.2147/IJN.S132780
- Stoker, T. B., Torsney, K. M., and Barker, R. A. (2018). "Pathological mechanisms and clinical aspects of GBA1 mutation-associated Parkinson's disease," in *Parkinson's Disease: Pathogenesis and Clinical Aspects*, eds T. B. Stoker and J. C. Greenland (Brisbane: Codon Publications).
- Tahaei Gilan, S. S., Yahya Rayat, D., Mustafa, T. A., Aziz, F. M., Shahpasand, K., Akhtari, K., et al. (2019). alpha-synuclein interaction with zero-valent iron nanoparticles accelerates structural rearrangement into amyloid-susceptible structure with increased cytotoxic tendency. *Int. J. Nanomed.* 14, 4637–4648. doi: 10.2147/IJN.S212387
- Teleanu, D. M., Chircov, C., Grumezescu, A. M., Volceanov, A., and Teleanu, R. I. (2018). Blood-brain delivery methods using nanotechnology. *Pharmaceutics* 10:269. doi: 10.3390/pharmaceutics10040269
- Terakawa, M. S., Lin, Y., Kinoshita, M., Kanemura, S., Itoh, D., Sugiki, T., et al. (2018). Impact of membrane curvature on amyloid aggregation. *Biochim. Biophys. Acta Biomembr.* 1860, 1741–1764. doi: 10.1016/j.bbmem.2018.04.012
- Uchimoto, T., Nohara, H., Kamehara, R., Iwamura, M., Watanabe, N., and Kobayashi, Y. (1999). Mechanism of apoptosis induced by a lysosomotropic agent, L-Leucyl-L-Leucine methyl ester. *Apoptosis* 4, 357–362. doi: 10.1023/A:1009695221038
- Uemura, N., Koike, M., Ansai, S., Kinoshita, M., Ishikawa-Fujiwara, T., Matsui, H., et al. (2015). Viable neuropathic Gaucher disease model in Medaka (*Oryzias latipes*) displays axonal accumulation of alpha-synuclein. *PLoS Genet.* 11:e1005065. doi: 10.1371/journal.pgen.1005065
- Vitali, M., Rigamonti, V., Natalello, A., Colzani, B., Avvakumova, S., Brocca, S., et al. (2018). Conformational properties of intrinsically disordered proteins bound to the surface of silica nanoparticles. *Biochim. Biophys. Acta Gen. Subj.* 1862, 1556–1564. doi: 10.1016/j.bbagen.2018.03.026
- Wang, C., Telpoukhovskaia, M. A., Bahr, B. A., Chen, X., and Gan, L. (2018). Endo-lysosomal dysfunction: a converging mechanism in neurodegenerative diseases. *Curr. Opin. Neurobiol.* 48, 52–58. doi: 10.1016/j.conb.2017.09.005
- Wood, S. J., Wypych, J., Stevenson, S., Louis, J. C., Citron, M., and Biere, A. L. (1999). alpha-synuclein fibrillogenesis is nucleation-dependent. Implications for the pathogenesis of Parkinson's disease. *J. Biol. Chem.* 274, 19509–19512. doi: 10.1074/jbc.274.28.19509
- Xie, H., and Wu, J. (2016). Silica nanoparticles induce alpha-synuclein induction and aggregation in PC12-cells. *Chem. Biol. Interact.* 258, 197–204. doi: 10.1016/j.cbi.2016.09.006

Conflict of Interest: The authors declare that the research was conducted in the absence of any commercial or financial relationships that could be construed as a potential conflict of interest.

Publisher's Note: All claims expressed in this article are solely those of the authors and do not necessarily represent those of their affiliated organizations, or those of the publisher, the editors and the reviewers. Any product that may be evaluated in this article, or claim that may be made by its manufacturer, is not guaranteed or endorsed by the publisher.

Copyright © 2021 Jiang, Gan, Yen and Dickson. This is an open-access article distributed under the terms of the Creative Commons Attribution License (CC BY). The use, distribution or reproduction in other forums is permitted, provided the original author(s) and the copyright owner(s) are credited and that the original publication in this journal is cited, in accordance with accepted academic practice. No use, distribution or reproduction is permitted which does not comply with these terms.